J. Biochem. 2011;150(4):395–402 doi:10.1093/jb/mvr062

JB THE JOURNAL OF BIOCHEMISTRY

Role of Asp187 and Gln190 in the Na^+/proline symporter (PutP) of *Escherichia coli*

Received March 25, 2011; accepted April 19, 2011; published online May 17, 2011

Anowarul Amin[1], Tadashi Ando[1,2], Shinya Saijo[1] and Ichiro Yamato[1,*]

[1]Department of Biological Science and Technology, Tokyo University of Science, 2641 Yamazaki, Noda-shi, Chiba 278-8510, Japan; and [2]Center for the Study of Systems Biology, School of Biology, Georgia Institute of Technology, Atlanta, GA 30318, USA

*Ichiro Yamato, Department of Biological Science and Technology, Tokyo University of Science, 2641 Yamazaki, Noda-shi, Chiba 278-8510, Japan. Tel: +81-4-7124-1501 (Ext 4405), Fax: +81-4-7125-1841, email: iyamato@rs.noda.tus.ac.jp

Asp187 and Gln190 were predicted as conserved and closely located at the Na^+ binding site in a topology and homology model structure of Na^+/proline symporter (PutP) of *Escherichia coli*. The replacement of Asp187 with Ala or Leu did not affect proline transport activity; whereas, change to Gln abolished the active transport. The binding affinity for Na^+ or proline of these mutants was similar to that of wild-type (WT) PutP. This result indicates Asp187 to be responsible for active transport of proline without affecting the binding. Replacement of Gln190 with Ala, Asn, Asp, Leu and Glu had no effect on transport or binding, suggesting that it may not have a role in the transport. However, in the negative D187Q mutant, a second mutation, of Gln190 to Glu or Leu, restored 46 or 7% of the transport activity of WT, respectively, while mutation to Ala, Asn or Asp had no effect. Thus, side chain at position 190 has a crucial role in suppressing the functional defect of the D187Q mutant. We conclude that Asp187 is responsible for transport activity instead of coupling-ion binding by constituting the translocation pathway of the ion and Gln190 provides a suppressing mutation site to regain PutP functional activity.

Keywords: coupling-ion binding/*Escherichia* coli/homology modelling/Na^+/proline symporter/transport activity.

Abbreviations: DM, Davis and Mingioli; HM, homology modelling; IPTG, isopropyl β-D-1-thiogalactopyranoside; MES, 2-(*N*-morpholino) ethanesulphonic acid; PAGE, polyacrylamide gel electrophoresis; PMS, phenazine methosulphate; SCF, sodium cotransporter family; SDS, sodium dodecyl sulphate; SSS, sodium solute symporters; TEV, tobacco etch virus; TM, transmembrane; WT, wild-type.

The high-affinity transport of proline is mediated by a secondary active transport system encoded by the *putP* gene (*1*). The transport of proline across the cytoplasmic membrane into cells is coupled with an electrochemical gradient of Na^+ or Li^+ (*2*, *3*). Based on sequence similarities, sodium/substrate transporters are grouped into different families (*4*), of which the sodium solute symporter (SSS) family comprises more than hundred members of prokaryotic and eukaryotic origin (*5*). The Na^+/proline symporter (PutP) of *Escherichia coli* is a well-characterized secondary active transporter, like SGLT (*6*) or NIS (*7*) and belongs to the SSS family (*5*).

PutP is an integral membrane protein (*2*) consisting of 502 amino acid residues with a molecular weight of 54,343 Da (*8*). This protein has been purified and characterized well to be responsible for Na^+/proline transport (*3*). The topology model has been proposed (*9*) and the mechanism of Na^+/proline symport was suggested to follow the ordered binding model (*10*, *11*).

In vitro site-directed mutagenesis has widely been used to study the structures and functions of PutP. Ser57 and Gly58 in the transmembrane region II (TM II) and Ser340 and Thr341 in the TM IX of PutP were shown to be important for high-affinity Na^+ and/or proline binding (*12*). Also, a carboxylate residue at position 55 of PutP was suggested to play a crucial role in coupling-ion binding (*13*). Asp187 located at the cytoplasmic loop between TM V and TM VI in the topology model of PutP was suggested to be important for uptake of proline and/or binding of coupling-ions (*14*). According to this study, an electrostatic interaction with the polar side chain of Asp187 was speculated to occur with the coupling-ion or other part of the transporter for active transport (*14*). In contrast, molecular dynamics simulation suggested that Asp189 in the SGLT of *Vibrio parahaemolyticus* (vSGLT), which corresponds to Asp187 in *E. coli* PutP (see below), was responsible not for coupling-ion binding but for facilitating the diffusion of the ion toward the cytoplasm (*15*).

Except vSGLT (PDB ID: 3DH4) of the SSS family (*6*), other membrane proteins including PutP have not yet been crystallized due to difficulties in crystallization. But three-dimensional (3D) structure is essential to elucidate the functional mechanism of a protein. Therefore, for unresolved proteins, homology model (HM) generated by various techniques could be useful to understand the structure/function relationship (*16*).

By multiple alignments of the amino acid sequences of PutP of *E. coli* with vSGLT and several members of the SSS family, we found that Asp187 of PutP is a conserved residue corresponding to Asp189 in vSGLT. We constructed a HM of PutP based on this multiple alignment and found Asp187 in the loop region near the Na^+ binding site with few other residues including the conserved adjacent Gln190.

Based on a previous analysis of Asp187 in PutP (*14*) and a recent molecular dynamics simulation of Asp189 in vSGLT (*15*), we re-examined the role of position 187 of PutP in more detail. We also gave attention to Gln190 of PutP because of its location near Na^+ in the HM structure.

Materials and Methods

Materials

DNA ligase and Taq polymerase were obtained from Takara Biotechnology Inc. (Kyoto, Japan). Synthetic oligonucleotides were from Operon Biotechnologies (Tokyo, Japan). The Benchmark protein ladder and Ni-NTA AP conjugate were purchased from Invitrogen life technologies (Tokyo, Japan) and QIAGEN (Tokyo, Japan), respectively. L-[U-^{14}C]-proline (246 mCi/mmol) was obtained from Moravex Biochemicals Inc. (CA, USA). Other chemicals were of reagent grade and obtained from Wako Chem. Co. (Osaka, Japan). The *E. coli* K-12 strain JM109 [*recA1*, *endA1*, *gyrA96*, *hsdRl7*, Δ(*lac-proAB*)/F′ (*traD36*, *proAB*′, *lacI*^{q} *ZΔM15*)] (*17*) and PT21recA [ST3009 (*proA*, *putC21*, *rpsL*, *putP21*, *proT*, *proP*), *recA*] (*1*, *3*) were used as recipients for transformation. The transport activity of proline in intact cells and the cytoplasmic membranes was measured using strain PT21recA harbouring various *putP* mutant plasmids. The PutP gene on pKHP1 (*18*) was excised and inserted into the HindIII–EcoRI sites of pUC19 under the control of the *lac* promoter/operator. Then a small DNA fragment containing a short linker, a tobacco etch virus (TEV) protease site and six His codons at the C-terminal tail followed a stop codon, TAA, was inserted at the C-terminal end of *putP* of this construct and named as pMYP. The *putP* was modified as introducing SacII in Leu181 [Leu (CTG) ⇒ Thr (ACC)] and SacI in Leu 371 [Leu (CTG) ⇒ Leu (CTC)] restriction sites at suitable positions in pMYP, which was renamed as pYAA1 and used as the parental wild-type (WT) plasmid for introducing various mutations into PutP.

Multiple sequence alignment

To determine those amino acid residues conserved among the sodium cotransporter family (SCF), multiple sequence alignments by the ClustalW (www.ebi.ac.uk/clustalw/), and LALIGN algorithms (www.ch.embnet.org/software/LALIGN_form.html) were used. With these tools, we also predicted the sequence similarity and identity of PutP and designed the HM structure.

Homology model

The crystal structure of the sodium/galactose symporter (SGLT) of *V. parahaemolyticus* has been solved. The predicted sequence similarity and identity of PutP with vSGLT were 57% and 18%, respectively (*6*). According to this and our multiple sequence alignment, we constructed a HM for PutP. Swiss-PdbViewer (V_4.01_PC) (*19*) and Accelrys Discovery studio 2.1 were mainly used for building the model. The structures were improved by using secondary structure prediction data methods (*20*) and previously published hydropathy data of this protein (*21*). A multiple alignment of Mhp1 (PDB ID: 2JLN) with PutP was also developed because Mhp1 exhibited 16% identity to vSGLT (*22*). We also utilized this alignment for an additional HM structure of PutP. After energy minimization by Swiss-PdbViewer, the obtained structures were processed to introduce Na^+, according to the coordinate of Na^+ in vSGLT after verifying the docking site in PutP using Discovery studio v2.1. Furthermore, according to multiple sequence alignments (Supplementary Fig. S1) and secondary structure model (*9*), we added the missing part of PutP TM I as a long α-helical extension (Supplementary Fig. S2), which was longer than other TM regions, by the help of bioinformatics tool (*20*) and Swiss-PdbViewer. Because of the highest similarity and identity with vSGLT and since Ala53, Met56, Ser340 and Thr341 (*12*) were the nearest to Na^+, a PutP HM based on vSGLT was finally chosen for our experiment.

Site-directed mutagenesis

Mutated constructs were individually obtained by site-directed mutagenesis utilizing the plasmid pYAA1 as a template. Nucleotide primers (Supplementary Table SI) having the desired mutations were used to obtain the specific mutated PCR products. The obtained fragments were excised by SacI and SacII and inserted into pYAA1 cut with the same restriction endonucleases. After ligation, both strands were verified by sequencing DNA [BigDye Terminator v3.1 (Applied Biosystem)] with an ABI 3130xl Genetic Analyzer.

Measurement of transport activity

The transport activities in intact PT21recA cells harboring various mutant plasmids were measured as described (*10*, *23*). According to these, cultivated and washed cells were suspended at 200 μg protein/ml with 50 mM Tris–MES (pH 7.0) (*23*, *24*). The uptake reaction (0.1 ml) was started by adding labelled 2 μM L-[U-^{14}C]-proline and 50 mM NaCl at 25°C to incubate for different time intervals (0–300 s) and was stopped by cold Davis and Mingioli (DM) minimal salt medium and the mixture was passed through a nitrocellulose filter. The radioactivity on the filter was measured with a liquid scintillation counting system (Beckman Coulter LS 6500). Three independent experiments were performed and the data were averaged. To estimate the apparent affinity for proline (K_m) and the maximum rate (V_{max}) of transport activity, the initial rate of L-[U-^{14}C]-proline uptake was measured in the presence of 50 mM NaCl using various concentrations of proline from 0.25 μM to 200 μM. For determination of the apparent affinity for Na^+, the proline concentration was fixed at 2 μM and NaCl concentration was varied from 0 mM to 2 mM. According to the Michaelis–Menten equation, K_m and V_{max} values were obtained using at least three independent experiments. Curve fitting and estimation of K_m and V_{max} were done with a software prism (GraphPad, San Diego, USA). We measured the contaminating Na^+ concentration in the reaction mixture using an atomic absorption spectroscopic flame emission spectrophotometer (SHIMADZU, AA6200). The highest concentration of the contaminating Na^+ was 3 μM in the Tris–MES buffer, which was considered in analysing the kinetic data.

Cytoplasmic membrane preparation and immunological analysis

Mutant PutPs were expressed using PT21recA as a host strain cultured in 1 l of casamino acid medium at 30°C with shaking (99 rpm). When the cell density, OD_{600}, was 0.6, IPTG (final concentration 0.2 mM) was added and cells were subjected to membrane preparation as described previously (*23*). The amount of protein was determined according to the Lowry method (*25*). Expression efficiency was compared between different mutants and WT PutP by loading same amounts of cytoplasmic membranes (20 μg) for SDS–PAGE. Gels were electroblotted on nitrocellulose membranes. A western blot analysis was performed using an alkaline phosphatase (AP) conjugated Ni-NTA to detect the His6-tag at the C-terminal end of the proline transporter (QIAGEN: Catalog 34510).

Binding activity of proline in membrane vesicles

The binding of proline to cytoplasmic membranes was measured using a microdialysis apparatus (*26*). The reaction mixture (100 μl) contained 250 μg of cytoplasmic membrane vesicles and 50 mM Tris–MES buffer (pH 6.5). To determine the binding affinity for proline, the NaCl concentration was fixed at 50 mM and 0.5–100 μM L-[U-^{14}C]-proline was used. On the other hand, to estimate the binding affinity for the coupling-ion Na^+, 2 μM L-[^{14}C]-proline was used with different concentrations of NaCl (0–100 mM). An uncoupler carbonyl cyanide *m*-chlorophenylhydrazone (10 μM) was included in the reaction mixture. The results were analysed according to a nonlinear regression plot using three individual experiments. Curve fitting and estimation of K_d were done with a software prism (GraphPad, San Diego, USA).

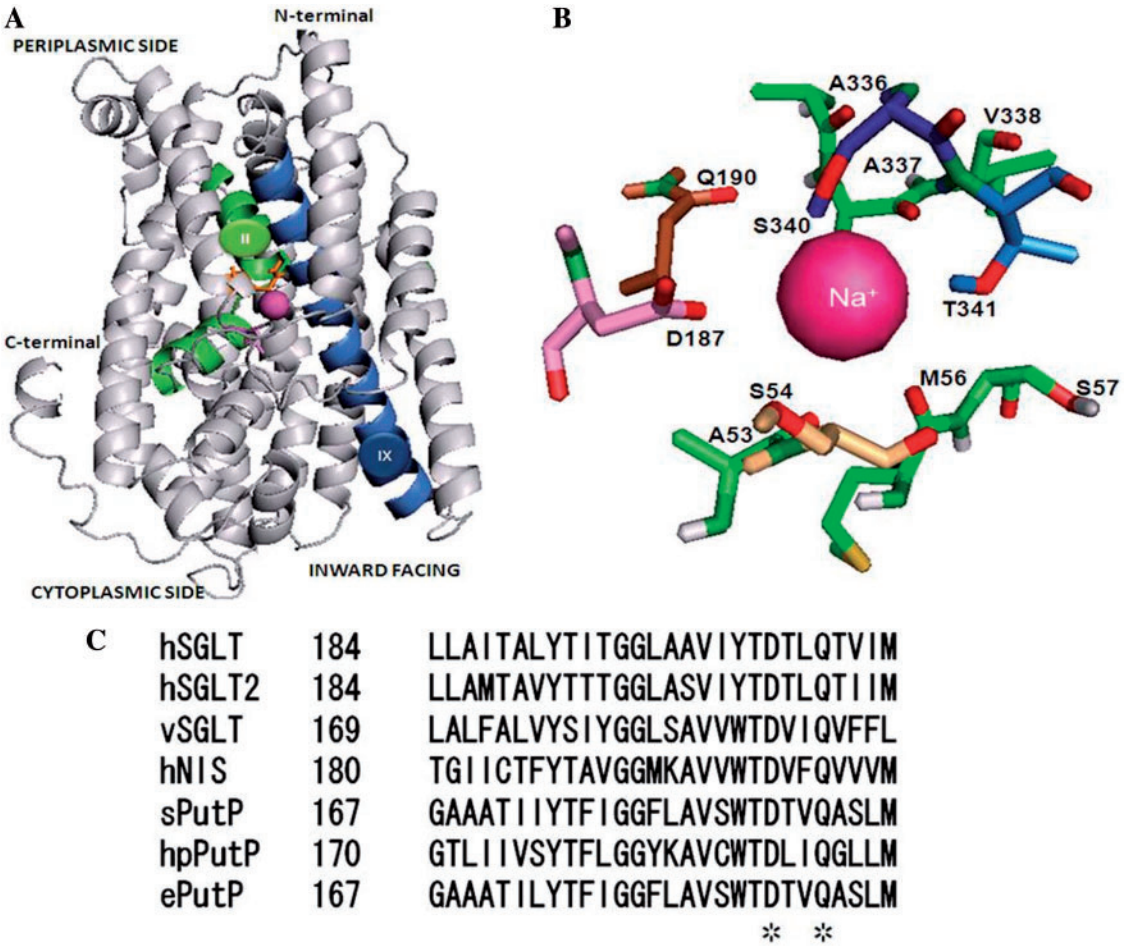

Fig. 1 The homology model structure and multiple sequence alignment of PutP. (A) The side chain of Asp187 (pink) and Gln190 (orange) were located at loop and TM regions, respectively in PyMol (DeLano Scientific) cartoon model. The TM region II and IX were shown in green and blue color, respectively, with the Na^+ (magenta sphere). (B) PyMol close-up view of the predicted Na^+ binding site and nearby residues with Asp187 and Gln190 within 6 Å of the Na^+ (magenta sphere) of PutP. (C) Multiple sequence alignments were performed using ClustalW. *Homo sapiens*, *V. parahaemolyticus*, *Salmonella typhimurium*, *E. coli* and *Helicobacter pylori* are indicated by prefixes h, v, s hp and e, respectively. The alignment shows the conserved (*) Asp187 and Gln190 of ePutP and the corresponding residues in other family members.

Results

Homology model

A brief description of the HM is included in the Supplementary Data (Supplementary Figs S1 and S2; Results section in Supplementary Data). Based on HM (Fig. 1A and B), predicted neighbouring residues (in Swiss-PdbViewer) within 6 Å of the coupling-ion Na^+ were Ala53, Ser54, Met56, Ser57, Asp187, Gln190, Ala336, Ala337, Val338, Ser340 and Thr341 (Fig. 1B). Ala53, Met56 in TM II and Ser 340, Thr341 in TM IX have been demonstrated to be important; but Ser54, Ser57 in TM II and Ala336, Ala337 and Val338 in TM IX have played no/less significant role in coupling-ion binding and/or active proline transport of PutP (*27*). Moreover, Asp187 was characterized as important for transport but its role in coupling-ion binding was conflicting because of its location not so close to the Na^+ as Ala53, Met56, Ser340 or Thr341 in the HM of PutP. In contrast, Gln190 was predicted to be within 6 Å of the coupling-ion though the role of this residue has not yet been investigated.

Multiple alignment of PutP

In alignment, Asp187 and Gln190 showed exceptional sequence conservation in SSS family (*4*, *5*). Except the Na^+/myoinositol symporter of *Canis familiaris* and Na^+/pantothenate symporter of *E. coli*, Asp187 was conserved in most of the known protein sequences and Gln190 showed sequence divergence only in the *E. coli* Na^+/pantothenate symporter. We thus characterized these two adjacent residues by site-directed mutagenesis to clarify the role (Fig. 1C).

Expression of Asp187/Gln190 mutants PutP

PutP expression and insertion into membranes were examined by western blotting (as shown in 'Materials and Methods' section). The proteins ran at the position of around 40 kDa, which corresponds to the calculated value of 55 kDa (*24*) (Fig. 2A) and the approximate protein contents in membranes were similar, suggesting no substantial effect on PutP protein expression.

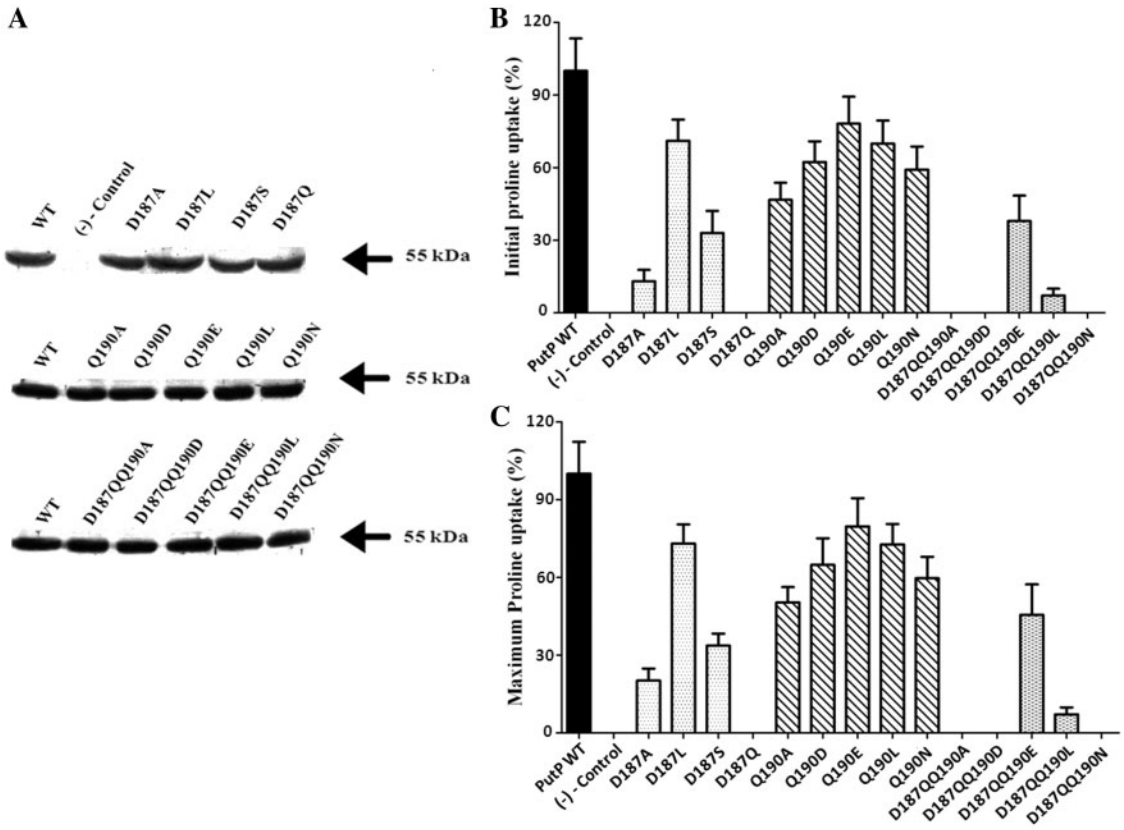

Fig. 2 Level of protein expression and effects of mutations on proline uptake of PutP. (A) Western blotting using cytoplasmic membranes (20 μg of protein) was done as described in 'Materials and Methods' section. A black arrow indicates the position of PutP. (B and C) The initial rate (B) (0–10 s) and maximum uptake (C) of proline uptake is represented as a percentage of the WT activity. The proline transport activity of PT21recA expressing the WT PutP protein was taken as 100% (solid bar). Each value represents the mean and standard deviation for at least three experiments. The initial rate and maximum uptake of WT PutP were 2.64 nmol/min/mg protein and 1.55 nmol/mg protein, respectively.

Proline transport activity of mutant cells

Under standard conditions, the initial uptakes by the D187L, D187S, D187A and D187Q mutants were 71, 33, 13 and 0% and maximum uptakes of 73, 34, 20 and 0%, respectively (Fig. 2B and C), compared with WT PutP. Replacement with Gln impaired the transport activity similar to that of PT21recA. Substitutions of Gln190 with other residues had no significant effect on PutP transport activity. The measured transport activities for the PutP Q190E, Q190L, Q190D, Q190N and Q190A mutants were 80, 73, 65, 60 and 50%, respectively, of WT PutP. It seems that the conserved Gln190 has no significant role in transport (Fig. 2C).

The inactive mutant D187Q was subjected to an additional substitution of Gln190 with Ala, Asn, Asp, Leu or Glu, same substitutions used to characterize the Gln190 single mutation as described above. The double mutants, D187QQ190A, D187QQ190N and D187QQ190D, showed no transport activity similar to the parental D187Q; whereas, a neutral Leu substitution at position 190 (D187QQ190L) resulted in 7% of the initial and maximum transport activity of the WT PutP. Interestingly, the Gln190 to Glu mutation in addition to D187Q, D187QQ190E, resulted in approximately half of the maximum proline transport of WT PutP (Fig. 2C). This result suggests that although Gln190 seemed apparently insignificant, the amino acid at position 190 is important for suppressing the inactivating mutation of D187Q as expected by its conservation and location close to the Na^+ binding site.

Proline transport properties of the mutants

We performed a kinetic analysis of the mutant cells as described in 'Materials and Methods' section. The summarized data were presented in Table I with the values of maximum velocity (V_{max}) and apparent K_m's for substrate and coupling-ion Na^+. The WT PutP showed the highest V_{max} with a K_m of 3.3 μM for proline while the mutants showed reduced V_{max} and apparently similar K_m's in the standard assay. Therefore, the substrate-specificity of these mutants was mostly similar to that of the WT (Fig. 3A and B), suggesting that none of the mutated amino acids played a major role in substrate binding. Furthermore, the estimated apparent K_m value of the WT PutP for Na^+ was 34 μM, similar to a previous report (*23*). As shown in Table I, the mutant Q190E showed the highest affinity for Na^+ ($K_{Na+} = 41$ μM) and D187QQ190L showed the lowest ($K_{Na+} = 68$ μM) affinity, suggesting not significantly different from the WT PutP (Fig. 3C and D). Thus, neither single nor double mutant PutP showed a significant alteration of the apparent affinity for the coupling-ion Na^+.

Table I. Kinetic values of proline transport activities of WT and mutant PutPs.

K_m and V_{max} values of WT and mutant PutPs											
PutP-D187	V_{max}[a]	K_m (Proline)[b]	K_m $(Na)^{+c}$	PutP-Q190	V_{max}[a]	K_m (Proline)[b]	K_m $(Na)^{+c}$	PutP-D187QQ190	V_{max}[a]	K_m (Proline)[b]	K_m $(Na)^{+c}$
WT	8.4 ± 0.22	3.3 ± 0.4	34 ± 8.0	Q190A	5.2 ± 0.24	6.5 ± 0.75	57 ± 9.0	D187QQ190A	[d]	[d]	[d]
D187A	3.0 ± 0.2	8.0 ± 1.6	64 ± 12	Q190D	5.4 ± 0.2	5.0 ± 0.68	52 ± 8.0	D187QQ190D	[d]	[d]	[d]
D187L	7.4 ± 0.32	4.5 ± 0.6	48 ± 10	Q190E	8.04 ± 0.37	4.0 ± 0.6	41 ± 9.0	D187QQ190E	5.3 ± 0.3	7.0 ± 1.0	53 ± 12
D187S	4.5 ± 0.15	6.0 ± 0.8	51 ± 13	Q190L	6.9 ± 0.3	4.5 ± 0.5	47 ± 8.0	D187QQ190L	1.2 ± 0.1	8.5 ± 2.7	68 ± 23
D187Q	[d]	[d]	[d]	Q190N	6.2 ± 0.25	5.0 ± 0.8	61 ± 10.0	D187QQ190N	[d]	[d]	[d]

The initial uptake activity of proline was measured using 20 μg of protein from intact cells as described in 'Materials and Methods' section. Apparent V_{max} and K_m values were calculated by fitting the data to the Michaelis–Menten equation using the nonlinear regression program (software prism 5). Data shown are means for three experiments. [a]V_{max} values for uptake are given in nmol/min/mg protein. [b]K_m value for proline and [c]K_m value for Na^+ are shown as μM. [d]Represents less than or close to negative control.

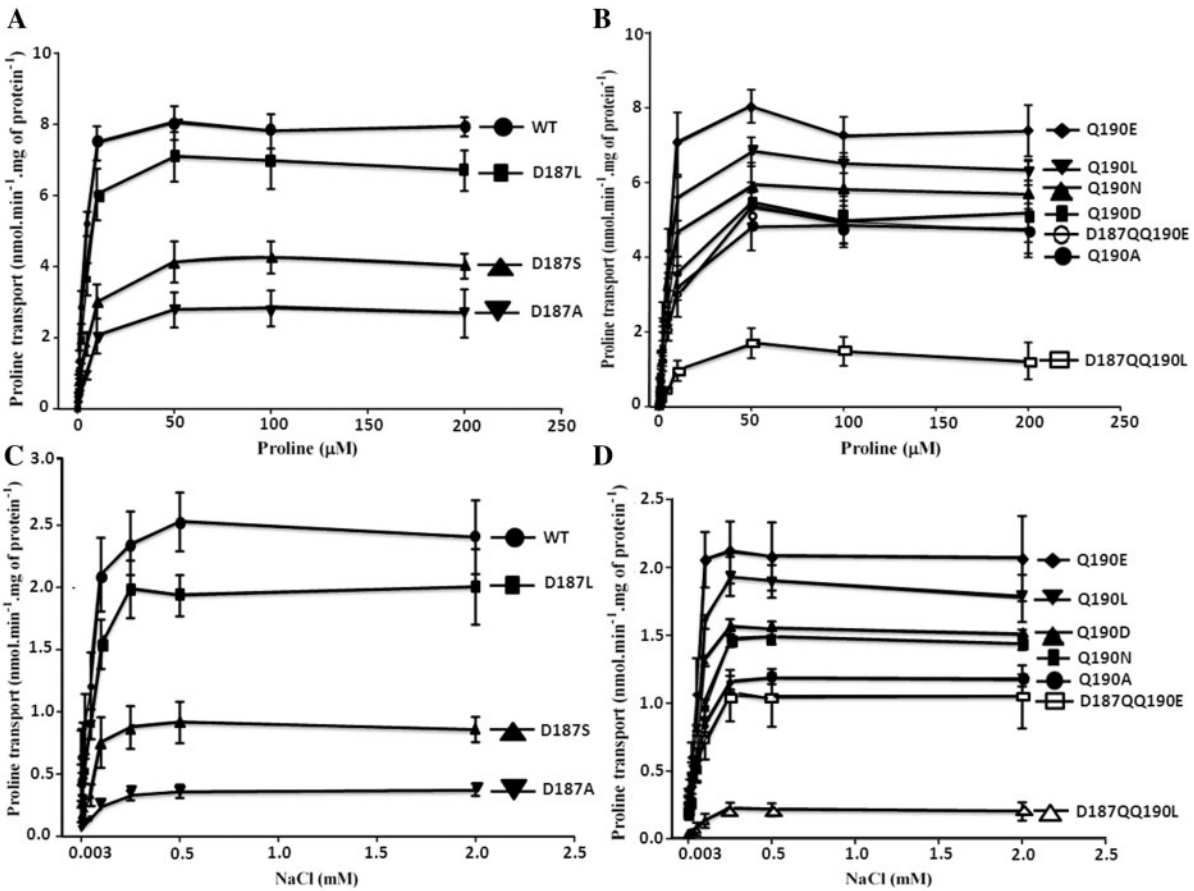

Fig. 3 Kinetics of the active transport of proline by various mutants. (A and B) Proline transport activity at various concentrations of proline in the presence of 50 mM NaCl. The initial uptake activity for proline was measured in triplicate using 20 μg of protein of intact cells. (C and D) Dependence on NaCl concentration of proline uptake activity in intact cells. The initial uptake activities in intact cells of WT and mutants were measured in the presence of 2 μM L-[U-^{14}C]-proline and different concentrations of NaCl as described in 'Materials and Methods' section. Kinetic values of transport were calculated using the Michaelis–Menten equation and presented in Table I. The Na^+ concentration in the buffer was 3 μM. Values are shown as the mean ± standard deviation ($n = 3$).

Binding properties of the mutants

As presented in Table II, the WT PutP showed maximum affinity for proline ($K_d = 6.5$ μM) and the highest of ~2-fold reduction in proline binding affinity was observed for the D187QQ190L mutant (Fig. 4A–C). Interestingly, the apparent affinity for proline of transport-negative mutants (Table I) did not differ markedly from the affinity of the WT PutP (Table II). Thus, it is clear that none of the mutants including D187Q changed the substrate binding properties. Asp187 and Gln190 were two conserved residues neighbouring Na^+ in the model of PutP; therefore, we measured the apparent affinity for the coupling-ion Na^+ (Fig. 4D–F). The inactive mutants also showed apparently similar affinities for Na^+, comparable to 6.0 mM of the WT (Table II), suggesting no substantial alteration in coupling-ion binding properties.

Table II. Binding affinity for proline and the coupling-ion Na^+ of WT and mutant PutPs.

	K_d values for proline and coupling-ion Na^+							
PutP-D187	**K_d (Proline)[a]**	**K_d (Na^+)[b]**	**PutP-Q190**	**K_d (Proline)[a]**	**K_d (Na^+)[b]**	**PutP-D187/Q190**	**K_d (Proline)[a]**	**K_d (Na^+)[b]**
WT	6.5 ± 0.8	6.0 ± 1.2	Q190A	10.0 ± 1.6	11.0 ± 2.5	D187QQ190A	12.0 ± 1.9	14.5 ± 3.4
D187A	11.0 ± 1.5	10.5 ± 2.6	Q190D	12.0 ± 1.7	11.5 ± 2.4	D187QQ190D	13.0 ± 2.7	13.5 ± 3.0
D187L	8.0 ± 1.3	9.0 ± 2.3	Q190E	9.5 ± 1.0	7.5 ± 1.2	D187QQ190E	10.0 ± 1.2	11.0 ± 2.0
D187S	9.5 ± 1.6	8.0 ± 2.0	Q190L	11.0 ± 1.3	8.5 ± 1.9	D187QQ190L	14.0 ± 2.0	13.0 ± 2.6
D187Q	10.0 ± 2.3	12.0 ± 3.0	Q190N	8.0 ± 1.1	10.0 ± 2.0	D187QQ190N	11.0 ± 1.9	12.0 ± 2.2

Specific binding activity was determined using membrane vesicles expressing WT and mutant PutP as described in 'Materials and Methods' section. The K_d's for proline and Na^+ were calculated using software prism5. [a]The K_d value for proline is shown in μM; [b]K_d value for Na^+ is shown in mM.

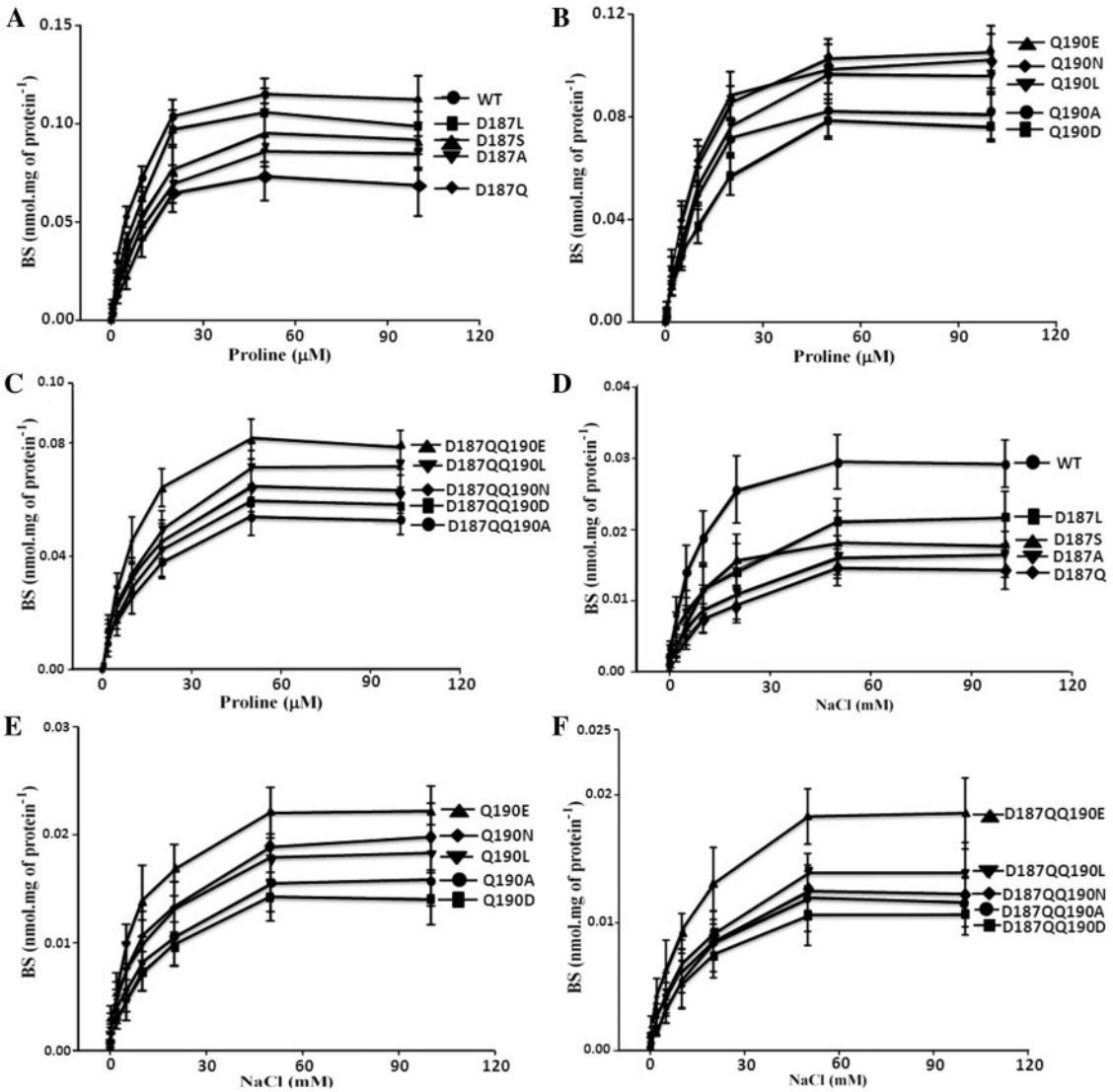

Fig. 4 Results of the equilibrium binding experiment of L-[U-^{14}C]-proline using membranes from WT and various mutants. (A–C) Membrane vesicles were incubated in the presence of increasing concentrations of L-[U-^{14}C]-proline and a fixed concentration of NaCl (50 mM) and the equilibrium binding was assayed as described in 'Materials and Methods' section. Data of specific binding, expressed as nmol bound/mg of protein (*Y*-axis), were plotted against the total ligand (S) concentration (*X*-axis). These curves were analysed by nonlinear regression. (D–F) NaCl concentration-dependence of specific proline binding activity in cytoplasmic membrane vesicles were measured in the presence of 2 μM L-[U-^{14}C]-proline with different concentrations of NaCl as described in 'Materials and Methods' section. A nonlinear regression curve was prepared for the proline bound to the cytoplasmic membrane vesicles (BS) against the total NaCl concentration. Error bars show the standard deviation of measurements estimated from three independent experiments. The calculated K_d values are presented in Table II.

Discussion

Previous study (*14*) showed that Cys at Asp187 inactivated the transport with exceptionally high affinity for coupling-ion Na^+, leading to high affinity for proline binding, while introducing Glu and Asn in place of Asp187 retained the transport and binding activities as WT PutP. In this study, we changed Asp187 to Ala, Leu, Ser and Gln and found that substitutions with Ala, Leu and Ser in place of Asp187 led to transport activities with similar affinity for substrate and coupling-ion compared with the WT PutP, suggesting the non-polar side chain at position 187 of PutP did not affect the transport or binding properties. Thus, it is probable that polar and non-polar residues work equally well and that side chain polarity at position 187 of PutP may not be important for maintaining the active proline transport process. Despite that electrostatic interactions by the side chain residue were proposed to play an important role in transport activity (*14*), adding Gln in place of Asp187 remarkably abolished the transport activity with no impairment in the binding of the substrate and/or coupling-ion Na^+. Since substitution of Asp187 to Asn or Glu did not affect the transport activity so much (*14*), it is probable that the mutation of Asp187 with Gln in PutP formed a specific interaction and/or conformation owing to the side chain property specific to Gln that blocked the release of Na^+ as well as proline towards the cytoplasm. Thus, we conclude that the side chain at position 187 of PutP is responsible for maintaining the transport activity rather than coupling ion binding, which is consistent with the prediction that Asp189 of vSGLT may not be the binding site of Na^+ (*15*).

As shown in the HM (Fig. 1A), Asp187 is located in a loop region and may be more flexible than in a helical part. A Na^+-induced conformational change was observed between positions 37 and 187 of PutP in *E. coli* (*28*). We, therefore, speculate that introducing Gln or Cys in place of Asp187 may have resulted in different interactions with other parts of the protein, which caused a possible conformational change in the loop region. The inward-facing conformation of vSGLT (*6*), outward-facing and occluded state of LeuT (*29*, *30*), and outward-facing, occluded and inward-facing conformations of Mhp1 (*22*, *31*). Therefore, we assumed that interaction of the side chain of Gln at Asp187 with other parts of PutP might have occurred in such a way that the protein can form an outward-facing conformation to bind proline and Na^+ like LeuT or Mhp1 but turned to a fixed conformation at inward-facing state (Fig. 1A) to interrupt the release of Na^+ and proline to accomplish active proline transport (*6*, *32*).

According to this speculation, we hypothesized that the deleterious interaction/conformational change brought about by Gln substitution at Asp187 may be recoverable by second site mutations at adjacent residues. As we mentioned, Gln190 is conserved and located close to Na^+ in HM, therefore, we introduced mutation at Gln190 of the D187Q mutant, since this Gln190 residue seems to orient in a similar direction as Asp187 in the HM (Fig. 1A). Surprisingly, D187Q PutP resumed to approximately half and 7% maximum transport activity of the WT PutP upon additional Q190E and Q190L mutations, respectively; while Ala, Asn and Asp substitutions had no effect. We modelled the side chain substitution at Gln190 in HM; side chains of Glu and Leu located close to the coupling-ion Na^+ and those of Ala, Asn and Asp were more distant than Glu and Leu. These results suggest that a subtle difference in the side chain interactions is important to maintain a favourable conformation for forming an active transport pathway of the coupling-ion. A cytoplasmic membrane protein TetC showed reduced efflux activity by Ser202 to Phe mutation but second site mutations of L11F, A213T and A270V suppressed the defect suggesting a similar mechanism of second site suppression (*33*). Thus, the position of Gln190 could also play an important role, restoring the transport activity of the inactive D187Q. In this respect, although it may be interesting to examine the suppression effect of Q190E second mutation on the D187C mutant reported by Quick and Jung (*14*), we do not think that Q190E shows similar suppressive effect since the mechanism of transport negative phenotype of D187C [very high affinity for Na^+ and proline; (*14*)] should be different from that of D187Q.

We conclude that Asp187 is located in the loop region and responsible for translocation instead of binding of the coupling-ion and the side chains of Asp187 and Gln190 may contribute to a conformation favourable for coupling-ion translocation. These results are consistent with our HM structure that served as a good starting model to study the structure/function of the Na^+/proline symporter.

Supplementary Data

Supplementary Data are available at *JB* online.

Acknowledgements

We thank Dr Satoshi Arai for suggestions during the experiments. We appreciate Dr Hiroyasu Seki for helping us in using the atomic absorption spectrophotometer.

Funding
The Ministry of Education, Culture, Sports, Science and Technology (MEXT), Japan.

Conflict of interest
None declared.

References

1. Mogi, T., Yamamoto, H., Nakao, T., Yamato, I., and Anraku, Y. (1986) Genetic and physical characterization of *putP*, the proline carrier gene of *Escherichia coli* K12. *Mol Gen Genet*. **202**, 35–41
2. Chen, C.C., Tsuchiya, T., Yamane, Y., Wood, J.M., and Wilson, T.H. (1985) $Na^+(Li^+)$-proline cotransport in *Escherichia coli*. *J. Membr. Biol*. **84**, 157–164

3. Hanada, K., Yamato, I., and Anraku, Y. (1988) Purification and reconstitution of *Escherichia coli* proline carrier using a site specifically cleavable fusion protein. *J. Biol. Chem.* **263**, 7181–7185
4. Reizer, J., Reizer, A., and Saier, M.H. Jr. (1994) A functional superfamily of sodium/solute symporters. *Biochim. Biophys. Acta.* **1197**, 133–166
5. Jung, H. (2002) The sodium/substrate symporter family: structural and functional features. *FEBS Lett.* **529**, 73–77
6. Faham, S., Watanabe, A., Besserer, G.M., Cascio, D., Specht, A., Hirayama, B.A., Wright, E.M., and Abramson, J. (2008) The crystal structure of a sodium galactose transporter reveals mechanistic insights into Na^+/sugar symport. *Science* **321**, 810–814
7. Dohan, O., De la Vieja, A., Paroder, V., Riedel, C., Artani, M., Reed, M., Ginter, C.S., and Carrasco, N. (2003) The sodium/iodide Symporter (NIS): characterization, regulation, and medical significance. *Endocr. Rev.* **24**, 48–77
8. Nakao, T., Yamato, I., and Anraku, Y. (1987) Nucleotide sequence of *putP*, the proline carrier gene of *Escherichia coli* K12. *Mol. Gen. Genet.* **208**, 70–75
9. Jung, H., Rubenhagen, R., Tebbe, S., Leifker, K., Tholema, N., Quick, M., and Schmid, R. (1998) Topology of the Na^+/proline transporter of *Escherichia coli*. *J. Biol. Chem.* **273**, 26400–26407
10. Yamato, I. and Anraku, Y. (1990) Mechanism of Na^+/proline symport in *Escherichia coli*: reappraisal of the effect of cation binding to the Na^+/proline symport carrier. *J. Membr. Biol.* **114**, 143–151
11. Yamato, I. (1992) Ordered binding model as a general mechanistic mechanism for secondary active transport systems. *FEBS Lett.* **298**, 1–5
12. Hilger, D., Bohm, M., Hackmann, A., and Jung, H. (2008) Role of Ser-340 and Thr-341 in transmembrane domain IX of the Na^+/proline transporter PutP of *Escherichia coli* in ligand binding and transport. *J. Biol. Chem.* **283**, 4921–4929
13. Quick, M. and Jung, H. (1997) Aspartate 55 in the Na^+/proline permease of *Escherichia coli* is essential for Na^+-coupled proline uptake. *Biochemistry* **36**, 4631–4636
14. Quick, M. and Jung, H. (1998) A conserved aspartate residue, Asp187, is important for Na^+-dependent proline binding and transport by the Na^+/proline transporter of *Escherichia coli*. *Biochemistry* **37**, 13800–13806
15. Li, J. and Tajkhorshid, E. (2009) Ion-releasing state of a secondary membrane transporter. *Biophys. J.* **97**, L29–31
16. Neve, K.A., Cumbay, M.G., Thompson, K.R., Yang, R., Buck, D.C., Watts, V.J., DuRand, C.J., and Teeter, M.M. (2001) Modeling and mutational analysis of a putative sodium-binding pocket on the dopamine D2 receptor. *Mol. Pharmacol.* **60**, 373–381
17. Sambrook, J., Fritsch, E.F., and Maniatis, T. (1989) *Molecular Cloning: A Laboratory Manual*. 2nd edn, Cold Spring Harbor Laboratory Press, Cold Spring Harbor, NY.
18. Hanada, K., Yamato, I., and Anraku, Y. (1987) Construction and properties of bifunctionally active membrane-bound fusion proteins. *Escherichia coli* proline carrier linked with beta-galactosidase. *J. Biol. Chem.* **262**, 14100–14104
19. Guex, N. and Peitsch, M.C. (1997) SWISS-MODEL and the Swiss-PdbViewer: an environment for comparative protein modeling. *Electrophoresis* **18**, 2714–2723
20. Soding, J. (2005) Protein homology detection by HMM-HMM comparison. *Bioinformatics* **21**, 951–960
21. Hanada, K., Yoshida, T., Yamato, I., and Anraku, Y. (1992) Sodium ion and proline binding sites in the Na^+/proline symport carrier of *Escherichia coli*. *Biochim. Biophys. Acta.* **1105**, 61–66
22. Weyand, S., Shimamura, T., Yajima, S., Suzuki, S., Mirza, O., Krusong, K., Carpenter, E.P., Rutherford, N.G., Hadden, J.M., O'Reilly, J., Ma, P., Saidijam, M., Patching, S.G., Hope, R.J., Norbertczak, H.T., Roach, P.C., Iwata, S., Henderson, P.J., and Cameron, A.D. (2008) Structure and molecular mechanism of a nucleobase-cation-symport-1 family transporter. *Science* **322**, 709–713
23. Yamato, I., Ohsawa, M., and Anraku, Y. (1990) Defective cation-coupling mutants of *Escherichia coli* Na^+/proline symport carrier. Characterization and localization of mutations. *J. Biol. Chem.* **265**, 2450–2455
24. Yamato, I., Kotani, M., Oka, Y., and Anraku, Y. (1994) Site-specific alteration of arginine 376, the unique positively charged amino acid residue in the mid-membrane-spanning regions of the proline carrier of *Escherichia coli*. *J. Biol. Chem.* **269**, 5720–5724
25. Peterson, G.L. (1977) A simplification of the protein assay method of Lowry et al. which is more generally applicable. *Anal. Biochem.* **83**, 346–356
26. Yamato, I. and Rosenbusch, J.P. (1983) Dependence on pH of substrate binding to lactose carrier in *Escherichia coli* cytoplasmic membranes. *FEBS Lett.* **151**, 102–104
27. Raba, M., Baumgartner, T., Hilger, D., Klempahn, K., Hartel, T., Jung, K., and Jung, H. (2008) Function of transmembrane domain IX in the Na^+/proline transporter PutP. *J. Mol. Biol.* **382**, 884–893
28. Jeschke, G., Wegener, C., Nietschke, M., Jung, H., and Steinhoff, H.J. (2004) Interresidual distance determination by four-pulse double electron-electron resonance in an integral membrane protein: the Na^+/proline transporter PutP of *Escherichia coli*. *Biophys. J.* **86**, 2551–2557
29. Yamashita, A., Singh, S.K., Kawate, T., Jin, Y., and Gouaux, E. (2005) Crystal structure of a bacterial homologue of Na^+/Cl^-dependent neurotransmitter transporters. *Nature* **437**, 215–223
30. Singh, S.K., Piscitelli, C.L., Yamashita, A., and Gouaux, E. (2008) A competitive inhibitor traps LeuT in an open-to-out conformation. *Science* **322**, 1655–1661
31. Shimamura, T., Weyand, S., Beckstein, O., Rutherford, N.G., Hadden, J.M., Sharples, D., Sansom, M.S., Iwata, S., Henderson, P.J., and Cameron, A.D. (2010) Molecular basis of alternating access membrane transport by the sodium-hydantoin transporter Mhp1. *Science* **328**, 470–473
32. Abramson, J., Smirnova, I., Kasho, V., Verner, G., Kaback, H.R., and Iwata, S. (2003) Structure and mechanism of the lactose permease of *Escherichia coli*. *Science* **301**, 610–615
33. Sapunaric, F.M. and Levy, S.B. (2003) Second-site suppressor mutations for the serine 202 to phenylalanine substitution within the interdomain loop of the tetracycline efflux protein Tet(C). *J. Biol. Chem.* **278**, 28588–28592